L. Sbita

M. Ben Hamed

JES

*Journal of
Electrical
Systems*

Internal Model Controller for Scalar Controlled Induction Motor Drive: Design and Experiments

This paper deals with the performance analysis and implementation of a robust speed controller. The robustness is guaranteed by the use of the internal model controller (IMC). Verification of the proposed robust controller is provided by experimental realistic tests on scalar controlled induction motor drives. Robust speed control at low speeds and in field weakening region is studied in order to show the robustness of the speed controller with a wide range of load

Keywords: Robust speed control, induction motor, scalar control, internal model control.

1. INTRODUCTION

Induction motors are relatively inexpensive and rugged machines. Consequently much attention has been given to induction motor control for starting, standstill, speed reversal, position control…etc. The induction motor torque is dependent both on the flux and the speed. But neither relationship is linear, a fact that complicates the design of the control system for induction machines. Thanks to scalar and Field orientation controls, induction machines are used for wide field of industrial applications [21].

Not only the coupling behavior of the induction motor consists a great problem but also the variation of their parameters mainly according to temperature [1]. Researchers have used various types of closed loop controllers for the rotor speed of the induction motor [18]. Among these controllers, the proportional integral derivative controllers are widely used in the outer speed loop. However, the use of this type of controller is more sensitive to parameter variation. To overcome this problem adaptive and robust control were used. The adaptive control imposes a very computation burden while H_∞ robust control requires the knowledge of the limit of the disturbance [7], [8] and [10]. The sliding mode control is also used in the speed loop but the most disadvantage of this type of controller is the high switching frequency [22]. Recently, speed controllers based on artificial intelligence techniques such as fuzzy logic and neural network based controllers have been proposed [5], [9], [13] and [20]. Since these approaches do not require the knowledge of a mathematical machine model, the algorithm would remains robust despite of parameter deviations and noises measurements. However, the computation expenses and the requirement of expert knowledge for the system setup have seriously restricted their applications in practice.

In this paper, an internal model controller is developed for the feedback of the scalar controlled induction motor. This IMC controller has the advantage of robustness, ease of design, good responses in transient state and in field weakening region. Details of the proposed IMC controller will be given in the following sections. Performance of the developed speed controller and its accuracy are verified by performing a series of experiments. These consist of step, acceleration, deceleration in low speeds and in field weakening region under both no load and loaded conditions.

Research Unity of Modeling, Analyze and Control Systems National Engineering School of Gabés (ENIG)- Tunisia. lassaad.sbita@enig.rnu.tn, benhamed2209@yahoo.fr

2. PROPOSED SCHEME OF THE DRIVE SYSTEM

The block diagram of the proposed induction motor drive system is shown in Figure 1. The closed loop control scheme of the induction motor is based on the internal model controller for the rotor speed [15]. The strategy to assume the decoupling of the induction motor is the scalar control using voltage source inverter [16] and [17].
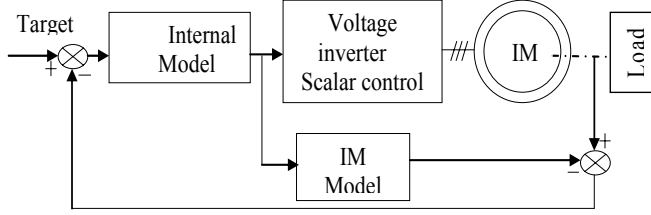

Figure 1: Block diagram of induction motor drive.

2.1 Scalar control induction motor

Scalar control strategy is designed based on the steady state operation. Based on the mathematical equations governing electrical dynamic of an induction motor in a synchronous rotating frame in the steady state, we obtain:

$$v_{ds} = r_s\, i_{ds} - \omega_s \Phi_{qs} \tag{1}$$

$$v_{qs} = r_s\, i_{qs} + \omega_s \Phi_{ds} \tag{2}$$

$$v_{dr} = r_r\, i_{dr} - (\omega_s - \omega)\Phi_{qr} \tag{3}$$

$$v_{qr} = r_r\, i_{qr} + (\omega_s - \omega)\Phi_{dr} \tag{4}$$

The d and q axis can be referred in a space vector if they are respectively placed at real and imaginary axis. Hence,

$$v_s = v_{ds} + j v_{qs} \tag{5}$$

$$i_s = i_{ds} + j i_{qs} \tag{6}$$

$$i_r = i_{dr} + j i_{qr} \tag{7}$$

$$\Phi_s = \Phi_{ds} + j\Phi_{qs} \tag{8}$$

$$\Phi_r = \Phi_{dr} + j\Phi_{qr} \tag{9}$$

Employing (1) and (2) in (5) yields:

$$v_s = r_s i_s + j\omega_s \Phi_s \tag{10}$$

Similarly, the rotor voltage is defined as:

$$v_r = r_r i_r + j\omega_r \Phi_r \tag{11}$$

The stator and rotor flux are:

$$\Phi_{ds} = L_s\, i_{ds} + M\, i_{dr} \tag{12}$$

$$\Phi_{qs} = L_s\, i_{qs} + M\, i_{qr} \tag{13}$$

$$\Phi_{dr} = L_r\, i_{dr} + M\, i_{ds} \tag{14}$$

$$\Phi_{qr} = L_r\, i_{qr} + M\, i_{qs} \tag{15}$$

Based on the equation system and equations (5)-(8), the stator and rotor flux in vector space are defined by:

$$\Phi_s = L_s\, i_s + M\, i_r \tag{16}$$

$$\Phi_r = L_r\, i_r + M\, i_s \tag{17}$$

By replacing the flux with their expressions, (10) and (11) become:

$$v_s = r_s i_s + j\omega_s [L_s\, i_s + M\, i_r] \tag{18}$$

$$0 = r_r i_r + j\omega_r [L_r\, i_r + M\, i_s] \tag{19}$$

In what follows, we use the well known equivalent single phase model transformed to the stator where we consider the magnetic leakages are totalized and grouped in the rotor and designed by $N_e\omega_s$ [12]. Figure 2 shows this model.
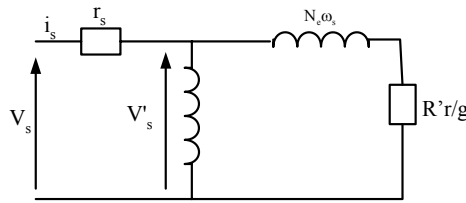

Figure 2: Single phase equivalent circuit of the induction machine.

where $R_r^{'}$ and N_e represent respectively the rotor resistance and total leakage inductance located in the rotor.

The evolution of the stator synchronous field round the rotor produces an electromagnetic power which will be transmitted to the rotor at synchronous speed. The electromagnetic power is defined as [19]:

$$P_{em} = T_{em}\Omega_s = 3\frac{R'_r}{g}\frac{V_s^2}{\left(\dfrac{R'_r}{g}\right)^2 + \left(N_e\omega_s\right)^2} \tag{20}$$

By assumption, we neglect the stator resistance and we obtain:

$$T_{em} = 6\pi\Phi_s^{\,2}\frac{\dfrac{R'_r}{f_r}}{\left(\dfrac{R'_r}{f_r}\right)^2 + \left(N_e 2\pi\right)^2} \tag{21}$$

where f_r is the slip frequency.

The mechanical dynamics of the induction motor is expressed as:

$$J\frac{d\omega}{dt} = p(T_{em} - T_L) \tag{22}$$

If we give the zero value to the load torque (T_L), the transfer function which defines the relation between the rotor speed ω and ω_s is given as:

$$\frac{\omega}{\omega s} = \frac{3p^2\Phi_s{}^2}{R'_r Js + (R'_r f + 3p^2\Phi_s{}^2)} = \frac{k}{1 + \tau s} \tag{23}$$

Here p is the number of poles pair, f is the viscous coefficient, τ is the time constant and k is the static gain of the system.

Hence, the scalar induction motor model is represented by a first order system. To identify the characteristics of this system model, a standard recursive least square (RLS) method is used.

2. 2 Identification with RLS algorithm

The recursive least square identification algorithm is described by the following steps [14]:

1. Initial conditions: the initial value of the estimated parameter vector $\widehat{\theta}$ is set equal to zero. The initial covariance matrix is assumed to be diagonal matrix with large positive numbers.

2. Compute estimate $\widehat{y}(k)$

$$\widehat{y}(k) = \widehat{\theta}^T(k-1)\mathrm{x}(k) \tag{24}$$

3. Compute the estimation error of $y(k)$

$$\varepsilon(k) = y(k) - \widehat{\theta}^T(k-1)\mathrm{x}(k) \tag{25}$$

4. Compute the estimation covariance matrix at instant k

$$P(k) = P(k-1) - \frac{P(k)\mathrm{x}(k)\mathrm{x}^T(k)P(k-1)}{1 + \mathrm{x}^T(k)P(k-1)\mathrm{x}(k)} \tag{26}$$

5. Compute the estimation vector at instant k

$$\widehat{\theta}(k) = \widehat{\theta}(k-1) + P(k)\mathrm{x}(k)\varepsilon(k) \tag{27}$$

6. Repeat 2-5 until the iteration number (measurement number) or the target error value is reached.

2.3 Induction motor model identification

The discreet induction motor model is defined as:

$$G(z) = \frac{\widehat{b}z^{-1}}{1 + \widehat{a}z^{-1}} = \frac{\widehat{y}(k)}{u(k)} \tag{28}$$

Based on (28), the recurrent equation is given as:

$$\widehat{y}(k) = \widehat{b}u(k-1) - \widehat{a}y(k-1) \tag{29}$$

This can be written as:

$$y(k) = \widehat{\theta}^{T}(k)\mathrm{x}(k) \tag{30}$$

$\widehat{\theta}$ is the vector of estimated parameters and x is the regression vector containing old inputs and outputs of the system to be identified.

Here $\widehat{\theta}$ and x are defined as:

$$\widehat{\theta}(k) = \begin{bmatrix} \widehat{b} & \widehat{a} \end{bmatrix}^{T} \tag{31}$$

$$\mathrm{x} = \begin{bmatrix} u(k\text{-}1) & \text{-}y(k\text{-}1) \end{bmatrix} \tag{32}$$

   To identify the estimated parameters, an experimental test was done on a 1kw induction motor scalar drive system. The drive is excited with a pseudo random binary sequence (PRBS) in order to obtain a data file input output measurements. An off line identification based on RLS is performed. The evolution of the output and input measurements are shown in Figure 3.
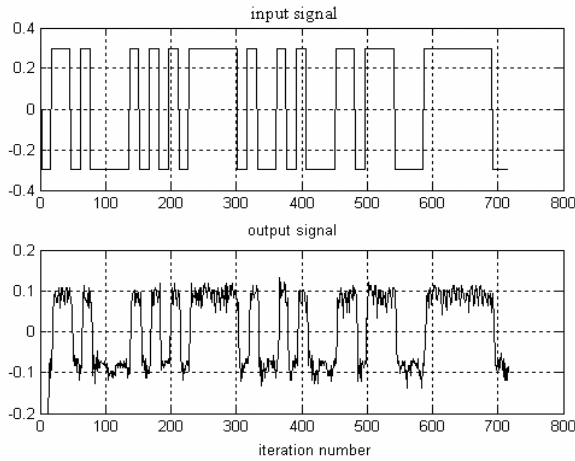

Figure 3: Evolution of the input and the output signals.

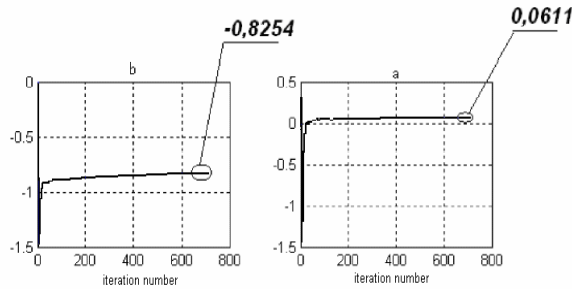The identification results are illustrated in Figure 4.

Figure 4: Evolution of the identification parameters.

Based on these results, the final discreet function can be written as:

$$Gm(z) = \frac{bz^{-1}}{1 + az^{-1}} = \frac{\omega(k)}{\omega_s(k)} \tag{33}$$

Where $b = 0.0611$ and $a = -0.8254$.

2.3 Validity of the established discreet induction motor model

The principle of this test is highlighted by these steps:

1. Compute the quantity defined as:

$$RN(i) = \frac{\sum\limits_{k=1}^{N} \varepsilon(k)\varepsilon(k-i)}{\sum\limits_{k=1}^{N} \varepsilon^2(k)} \ , \text{if } i \succ 1. \tag{34}$$

$i = \sup(-n_a, n_b + d)$ with n_a is the order of the denumerator and n_b is the order of the numerator.

2. Verify the condition validity given as:

$$|RN(i)| \leq \frac{2,17}{\sqrt{N}} \tag{35}$$

In our application $N = 716$. Then, we get $|RN(i)| \leq 0,0811$.

The theoretical computation leads to:

$$RN(0) = 1,$$
$$RN(1) = -0.0733,$$
$$RN(2) = -0.0544,$$
$$RN(3) = -0.0466. \tag{36}$$

As shown by these results, the condition (35) is already verified. Therefore, we conclude that the established induction motor model is valid.

2.4 Internal model controller

The speed controller is based on the principle of internal model control which makes it robust and immune to disturbances (parameter variations and external load torque disturbance) [2] and [3]. The internal model controller is consisting of mainly the controller and the discreet system model. The block diagram of the structure of internal model controller is given in Figure 5.

When the process is linear and so as, it can be described by a transfer function $G(z)$, based on the bloc diagram of the internal model controller (Figure 5), we establish:
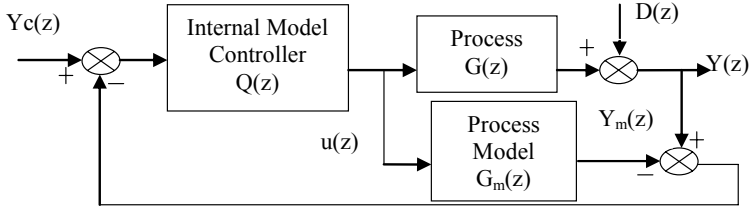
Figure 5: Block diagram of internal model control.

$$y(z) = G(z)\,u(z) + D(z) \tag{36}$$

$$ym(z) = Gm(z)\,u(z) \tag{37}$$

The command $u(z)$ is expressed as:

$$u(z) = Q(z)\Big[\big[yc(z) - (G(z) - Gm(z))u(z)\big] - D(z)\Big] \tag{38}$$

It can be simplified as:

$$u(z) = \Big[1 + Q(z)(G(z) - Gm(z))\Big]^{-1} Q(z)\big[yc(z) - D(z)\big] \tag{39}$$

where $yc(z)$ denotes the target value of the output value $y(z)$.

By replacing $u(z)$ with its value in (36) yields

$$y(z) = G(z)\Big[1 + Q(z)(G(z) - Gm(z))\Big]^{-1} Q(z)\big[yc(z) - D(z)\big] + D(z) \tag{40}$$

Here, we distinguish two circumstances:

• We suppose that the modeling system is perfect. Therefore $G(z) = Gm(z)$. Using this condition, we obtain:

$$y(z) = G(z)\,Q(z)\big[yc(z) - D(z)\big] + D(z) \tag{41}$$

The aim is to assume that $y(z) = y_c(z)$ in steady state in tracking and regulation. It is clear that if we choose $Q(1) = G(1)^{-1}$, then $y(\infty) = y_c(\infty)$ if k converges to ∞. The writing $Q(1) = G(1)^{-1}$ is possible only if the process is stable.

• Now, the modeling process is not perfect. To eliminate the effect of the modeling error, a low pass filter $F(z)$ is added. In this case:

$$y(z) = G(z)\Big[1 + Q(z)F(z)(G(z) - Gm(z)\Big]^{-1} Q(z)\big[yc(z) - F(z)D(z)\big] + D(z) \tag{42}$$

From this equation, it is clear that to eliminate the disturbance and to assume $y(\infty) = y_c(\infty)$ if k converges to ∞, we must choose $Q(1)F(1)Gm(1) = 1$. The easy way is to choose a low pass filter with a unit static gain.

In practice, the low pass filter is used not only to eliminate the modeling error but also to make the controller physically realized. It has an adjustable parameter. This adjustable parameter can be adjusted on line and off line in order to make the internal model controller

more robust about modeling errors. Hence, the final form of the internal model controller is given as:

$$Q(z) = Q_0(z)F(z) \tag{43}$$

The model internal controller is applied for only stable system.

To obtain the final form of the internal model controller, five steps are to be followed:

Step 1: the zeros of $Q_0(z)$ are the poles of the model system.

Step 2: the poles of $Q_0(z)$ are chosen as

- the stable zeros of the model system,
- the reverse of the instable zeros of the model system,
- a pole zero is added at each zero with a negative real part,

Step 3: a pole zero is added to $Q_0(z)$,

Step 4: to obtain a zero error in the steady state, the controller gain is chosen so that $Q_0(1)G(1) = 1$,

Step 5: a low pass filter is added in order to overcome the problems caused by the modeling error. In general [4] and [6]:

$$F(z) = \frac{(1-\alpha)z}{z-\alpha} \tag{44}$$

where $0 < \alpha < 1$.

The robustness of this controller is achieved by a good choice of the coefficient α.

The final form of the IMC controller can be written as:

$$Q(z) = Q_0(z)F(z) \tag{45}$$

Now, in order to determinate $u(k)$, we calculate the product between $F(z)$ and $u_0(k)$. Therefore, we obtain:

$$u(k) = F(z)u_0(k) \tag{46}$$

Replacing $F(z)$ with its value, (46) yields

$$u(k) = \alpha u(k-1) + (1-\alpha)u_0(k) \tag{47}$$

If α is nearby 1 ($1-\alpha$ converges to zero), then, $u(k)$ remains nearby $u(k-1)$ although the difference process model occurs which prove the robustness of this controller. Hence the process dynamic in closed loop is fixed by this filter parameter. A several experimental tests were carried to tune the filter parameter with respect to the compromise between rapidity and stability of the overall system. The final value used is then fixed to 0.9.

The condition of the internal model control is justified by the Nyquist locality shown in Figure 6. Based on the Nyquist criterion which announce that a necessary and sufficient stability condition is that the round number of Nyquist diagram round the critical point $(-1,0)$ in direct direction have to be equaled to instable zero number of his transfer function in open loop. In our application, the transfer function in open loop has no instable

zero and as given in Figure 6, its Nyquist diagram doesn't turn round the critical point (-1, 0) in direct direction. Therefore, based on this criterion, the induction motor model is sable. Hence, the IMC can be used in the control loop.
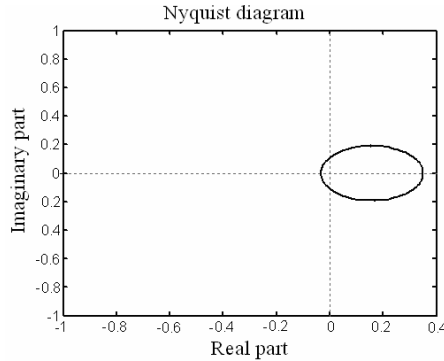

Figure 6: Nyquist locality of the induction motor open loop transfer function.

Based on these five steps, the internal model controller is obtained as

$$u(k) = b_0 e(k-1) + b_1 e(k-2) + a_0 u(k-1) \tag{47}$$

where e is the error between real output and model output, $a_0 = \alpha$, $b_0 = \dfrac{1-\alpha}{a}$ and

$b_1 = \dfrac{(1-\alpha)b}{a}$.

3. EXPERIMENTAL RESULTS

The experimental setup is shown in figure 7. It consists of appropriate hardware and its software implemented through a processor based digital controller. The major parts of the drive system are:

- IMC Speed controller,

- Inverter drive,

- A power inverter based on the IGBT transistors and L, C filter,

- Scalar control set around a micro-controller,

- Pc with an acquisition and control card $(\pm 10v)$,

- Induction motor (1kw-4.6A) coupled to DC generator (1kw-6.2A) supplying a variable resistive load.

Some of them are implemented through software and are namely IMC speed controller. The remaining parts are implemented using the developed hardware.

Many experiments were carried out on the various operating conditions to verify the performance of the proposed internal model speed controller (low speed operation, reverse operation, field weakening region…etc.) under no load and load applied. Some selected results are presented in this section to highlight the significant operating conditions for the proposed system.

Figure 7: Experimental setup.

Figures 8 and 9 show speed responses under constant load of 400w and 200zm respectively. Figures 10-11 show, respectively, the step responses for 700rpm and 2000rpm with different selected resistive applied load about 400W and 200W. These results justify the robustness of the overall control system under parameter variation and load disturbances.

In Figure 11, a wide range of selected resistive load is considered and applied in order to test the robustness of the proposed control algorithm. In this test, both the field weakening operation and load torque disturbance are considered. Hence, high speeds require rather large input voltages. In practice, the voltage must be kept within the inverter ceiling limits [11] so that the flux is decreased from the rated as the speed increases above rated one (scalar law strategy at constant power). This method of reducing the flux at high speeds is called "field weakening". It can be noted that at a high speed of 1800rpm, the control system achieve a good disturbance rejection and stability. The system power limitation explains the speed droop occurring at 19s.
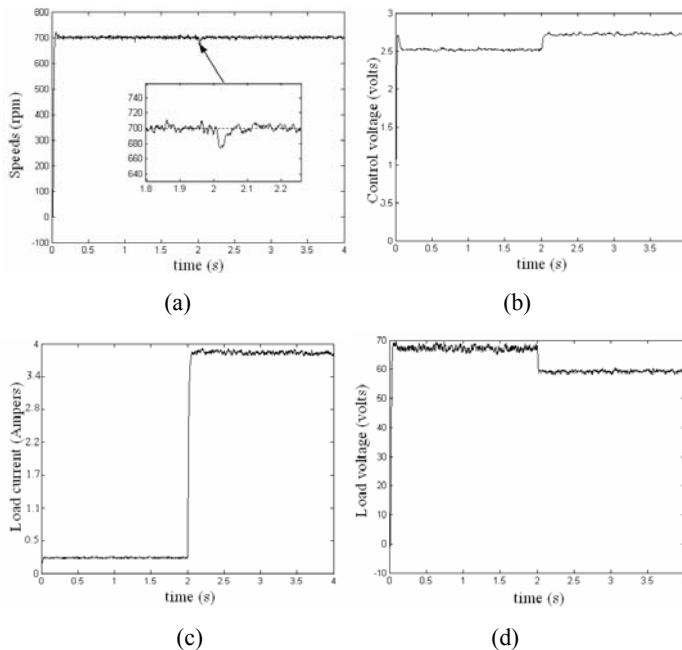

(a)

(b)

(c)

(d)

Figure 8: Speeds, control voltage, load current and voltage responses under constant load of 400w
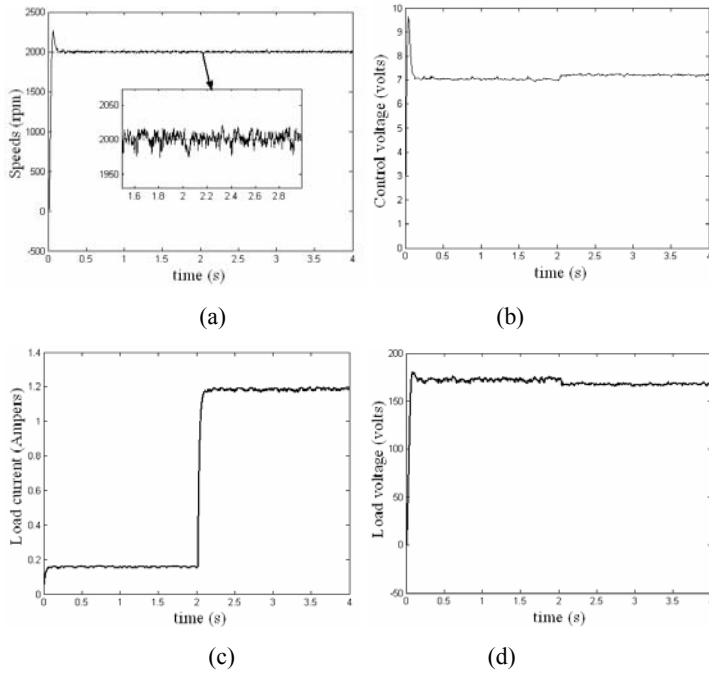
(a)

(b)

(c)

(d)

Figure 9: Speeds, control voltage, load current and voltage responses under constant load of 200 w
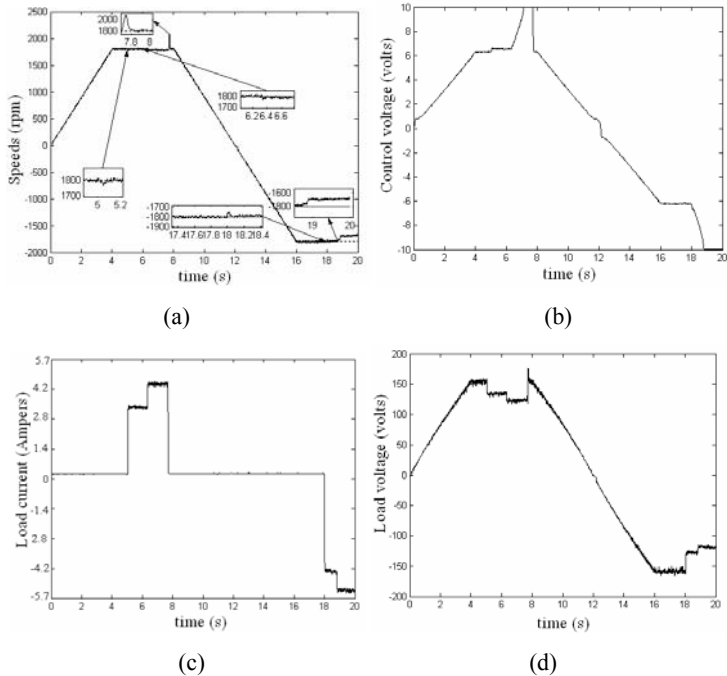

(a)

(b)

(c)

(d)

Figure 10: Speeds, control voltage, current and load responses under variable load of 350 w at t=5s, 450 w at t=6s no load at t=8s, 450w at t=18s and 550 w at t=19s (variable target speed as acceleration and deceleration).
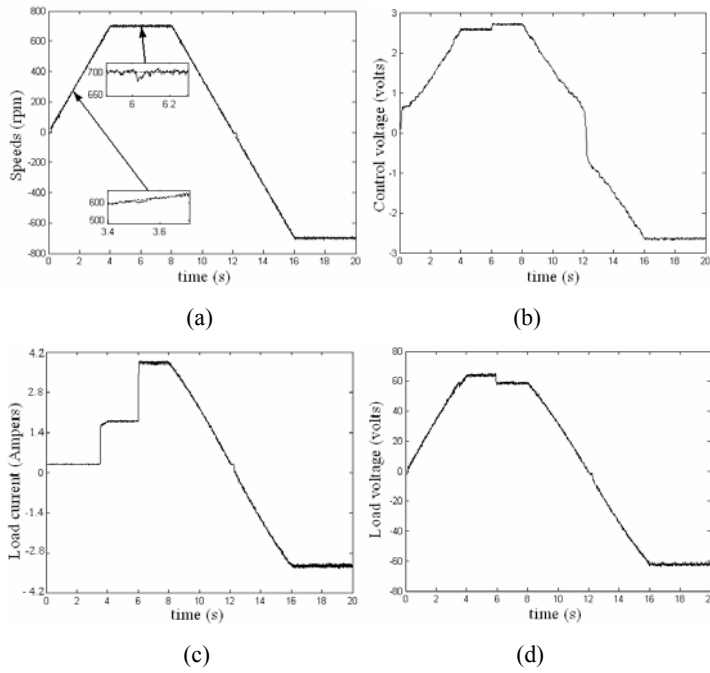
(a)   (b)

(c)   (d)

Figure 11: Speed, control voltage, load current and load voltage responses of speed IMC controller under constant load of 200 w at t=3.5s and 0.5 kw at t=6s (variable target speed as acceleration and deceleration).

The tests of the algorithm under no load are given in figures 12 to 17. Low speed, field weakening region and reverse operation are all of studied then tested experimentally. From these figures, it is seen that the proposed control algorithm has good performance and stability.
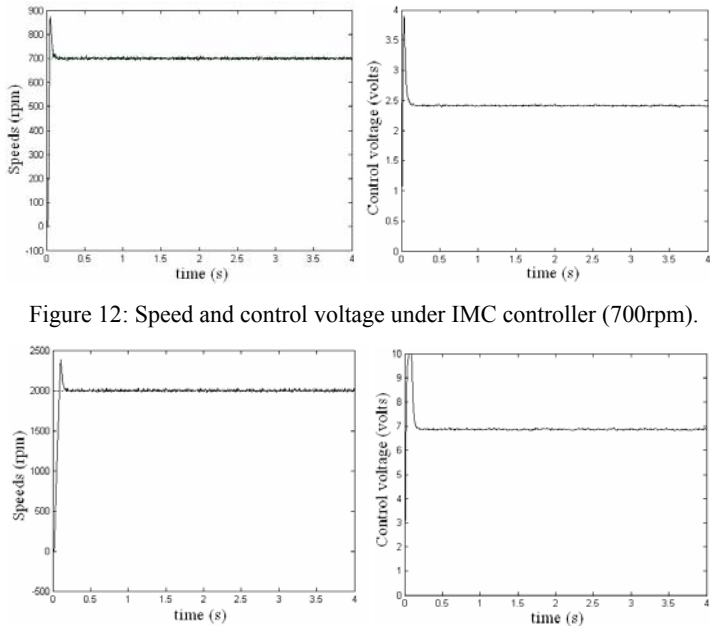

Figure 12: Speed and control voltage under IMC controller (700rpm).
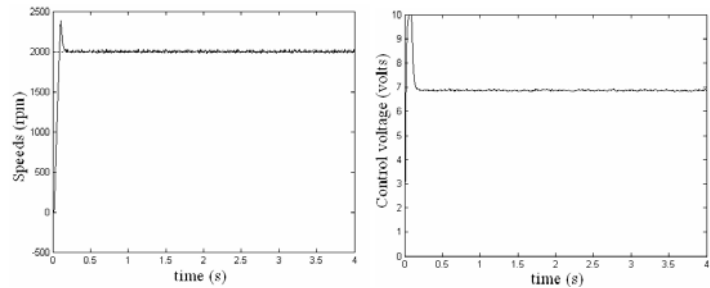

Figure 13: Speed and control voltage under IMC controller (2000rpm: field weakening region).
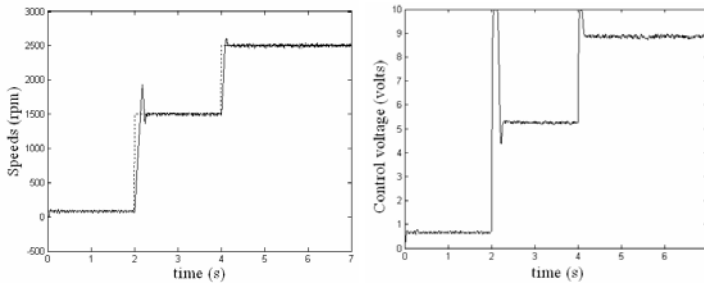
Figure 14: Speed and control voltage under IMC controller (variable target speed).
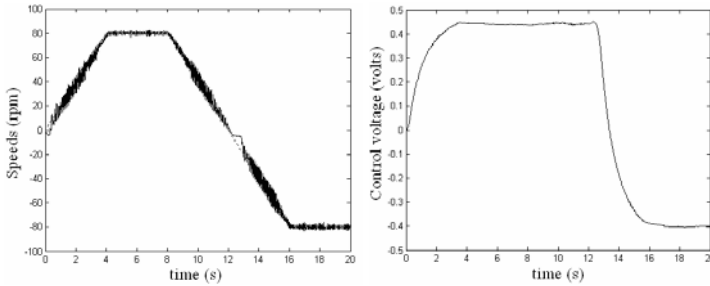

Figure 15: Speed and control voltage under IMC controller (variable low target speed: permanent target speed of ±80rpm).
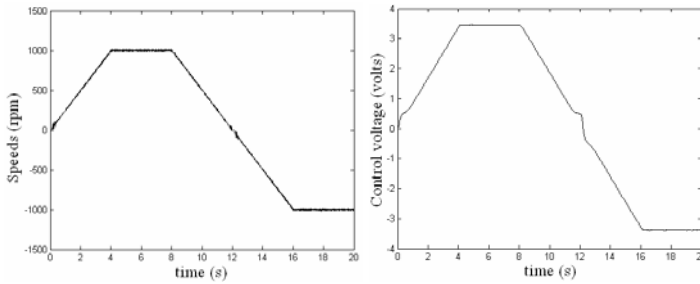

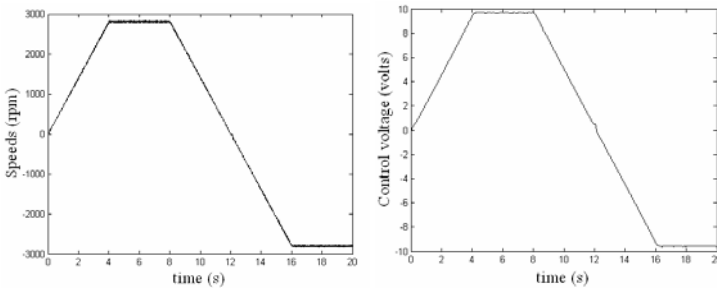Figure 16: Speed and control voltage under IMC controller (variable target speed ±1000rpm).

Figure 17: Speed and control voltage under IMC controller (variable target speed: field weakening region, permanent target speed of ±2800rpm).

4. CONCLUSION

In this paper, an internal model speed controller for induction motor is designed and implemented for a scalar induction motor drives system. An identification methodology

based on the recursive least square algorithm is successfully applied in this work to identify the parameters of the established mathematical model of the drive system. From the experimental results using a 1kw induction motor drive system, it is shown that the proposed speed controller over the entirely speed range and under a wide range of load has a good performance and stability. The most important advantage of the proposed algorithm is to provide a robust structure and a simple and easy design compared to other methods.

Due to the drawbacks of the speed sensorless, a simple speed estimator based on the generation of the controller signal in one hand and an artificial neural networks observer on the other hand and the torque optimization could be the subject of future follow up research work.

REFERENCES

[1] C. Mastorocostas, I. Kioskeridis and N. Margaris, Thermal and slip effects on rotor time constant in vector controlled induction motor drives, IEEE Trans. Power Electron., vol. 21, no. 2, pp. 495 – 504, Mar. 2006.

[2] X. Shao, J. Zhang, Z. Zhao and X. Wen, Adaptive internal Model Control of Permanent Synchronous Motor Drive System, in Proc. Electrical Machines and Systems, ICEMS 2005, vol. 3, pp. 1843-1846, Sept. 2005.

[3] A. M. Segayer and A. M. Jaroushi, Competitive co-evolutionary design of robust internal model controllers to deal with prescribed large plant uncertainties. Presented at SSD'2005.

[4] P. Borne, G. D. Tongy, J. P. Richard, F. Rotella and I. Zambettakis, Commande et Optimisation des Processus. Paris: Technip, 1998.

[5] L. Sbita and M. Ben Hamed, Fuzzy controller and ANN speed estimation for induction motor drives. Presented at SSD'2007.

[6] J. M. Flaus, Régulation Industrielle: Régulateurs PID, Prédictifs et Flous. Paris: Hermès, 2000.

[7] G. Duc and S. Font, Commande H_∞ et μ – analyse. Paris: Hermès, 1999.

[8] A. Oustaloop, La Robustesse: Analyse et Synthèse des Commandes Robustes. Paris: Hermès, 1994.

[9] O. Omidvar and D. L. Elliott, Neural systems for control. New York: Academic Press, 1997.

[10] Y. Ben Salem et L. Sbita, Synthèse H_∞ Loop shaping appliquée à la commande vectorielle d'un actionneur asynchrone sans capteur de vitesse. Presented at IEEE JTEA'2006. [CD - ROM].

[11] Y. Ben Salem and L. Sbita, A Nonlinear state feedback control for induction motors, Presented at IEEE. ICIT'2006. [CD - ROM].

[12] G. Grellet and G. Clerc, Actionneurs Electriques, Paris: Eyrolles, 1996.

[13] M. A. Denai and S. A. Attia, Fuzzy and Neural Control of an Induction Motor, Int. J. Appl. Math. Comput. Sci., Vol. 12, no. 2, pp. 221- 223, 2002.

[14] Y. Koubaa, Recursive identification of induction motor parameters, Int. J. Simulation Modeling Practice and Theory, 12, pp. 363–381, 2004.

[15] A. Jaime., A. Joaquin and R. J. Herrera, Internal model control for non linear systems: application to an induction motor, Int. J. Control Engineering Practice, Vol. 2, no. 6, pp. 1063 – 1066, Dec. 1994.

[16] F. Zidani, M. S. Nait Said, R. Abdessemed, D. Diallo and M. E. H. Benbouzid, A Fuzzy Technique for Loss Minimization in Scalar-Controlled Induction Motor, Electric Power Components and Systems, vol. 30, pp. 625-635, 2002.

[17] A. M. Garcia, T. A. Liop and D. W. Novotny, A new induction motor V/f control method capable of high-performance regulation at low speeds, IEEE Trans. Ind. Applicat., vol. 34, no. 4, pp. 813-821, Jul.-Aug. 1998.

[18] J. Holtz, Sensorless Speed and Position Control of Induction Motor Drives, In Proc. 27th Annu. Conf. IEEE Industrial Electronics Society IECON'01, Denver, Colorado, 2001, pp. 1554-1562.

[19] I. Boldea and S. A. Nasar, Electric Drives, Taylor and Francis Group, 2005.

[20] J. Fonseca, J. L. Afonso, J. S. Martins and C. Couto, Fuzzy logic speed control of an induction motor, Int. J. Microprocessors and Microsystems, 22, pp. 523–534, 1999.

[21] H. M. B. Metwally, Proposed torque optimized behaviour for digital speed control of induction motors, Int. J Energy Conversion & Management, 43, pp. 1675–1688, 2002.

[22] C. K. Lai and K. K. Shyu, A novel motor drive design for incremental motion system via sliding –mode control method, IEEE Trans. Power Electron., vol. 52, no. 2, pp. 7-30, Apr. 2005.